

LATTICE BOLTZMANN SIMULATION OF MAGNETIC FIELD DIRECTION EFFECT ON NATURAL CONVECTION OF NANOFLUID-FILLED CAVITY

Ahmed Mahmoudi¹, Imen Mejri¹, Mohamed Ammar Abbassi¹ and Ahmed Omri¹

¹UR:Unité de Recherche Matériaux, Energie et Energies Renouvelables (MEER), Faculté des Sciences de Gafsa, B.P.19, Zarroug, Gafsa, 2112, Tunisie

ABSTRACT

This paper examines the natural convection in a square enclosure filled with a water-Al₂O₃ nanofluid and is subjected to a magnetic field. The bottom wall is uniformly heated and vertical walls are linearly heated whereas the top wall is well insulated. Lattice Boltzmann method (LBM) is applied to solve the coupled equations of flow and temperature fields. This study has been carried out for the pertinent parameters in the following ranges: Rayleigh number of the base fluid, Ra=10³ to 10⁵, Hartmann number varied from Ha=0 to 60, the inclination angle of the magnetic field relative to the horizontal plane $\gamma = 0^\circ$ to 180° and the solid volume fraction of the nanoparticles between $\phi = 0$ and 6%. The results show that the heat transfer and fluid flow depends strongly upon the direction of magnetic field. In addition, according the Hartmann number, it observed that the magnetic field direction controls the effects of nanoparticles.

1. Introduction

The problem of natural convection in square enclosures has many engineering applications such as: cooling systems of electronic components, building and thermal insulation systems, built-in-storage solar collectors, nuclear reactor systems, food storage industry and geophysical fluid mechanics [1]. Some practical cases such as the crystal growth in fluids, metal casting, fusion reactors and geothermal energy extractions, natural convection is under the influence of a magnetic field [2-3]. Badawi et al. [4] studied numerically MHD natural convection iso-flux problem inside a porous media filled inclined rectangular enclosures. The results show that both the magnetic force and the inclination angle have significant effect on the flow field and iso- heat flux in porous medium. Abishek et al. [5] studied numerically natural convection of an electrically conducting fluid due to both heat and solutal transfer, in a square enclosure filled with porous medium, subjected to a uniform magnetic field applied parallel to the adiabatic walls on the plane of the enclosure. It is found that the effect of the applied magnetic field is significant to the extent that convection is completely suppressed for large values of Ha. Fattahi et al. [6] applied Lattice Boltzmann Method to investigate the natural convection flows utilizing nanofluids in a square cavity. The fluid in the cavity was a water-based nanofluid containing Al₂O₃ or Cu nanoparticles. The results indicated that by increasing solid volume fraction, the average Nusselt number increased for both nanofluids. It was found that the effects of solid volume fraction for Cu were stronger than Al₂O₃. Kefayati et al. [7] simulated by the Lattice Boltzmann method the natural convection in enclosures using water/SiO₂ nanofluid. The results showed that the average Nusselt number increased with volume fraction for the whole range of Rayleigh numbers and aspect ratios. Also the effect of

nanoparticles on heat transfer augmented as the enclosure aspect ratio increased. Lai and Yang [8] performed mathematical modeling to simulate natural convection of Al₂O₃/water nanofluids in a vertical square enclosure using the Lattice Boltzmann method. The results indicated that the average Nusselt number increased with the increase of Rayleigh number and particle volume concentration. The average Nusselt number with the use of nanofluid was higher than the use of water under the same Rayleigh number. Mahmoudi et al. [9] presented a numerical study of natural convection cooling of two heat sources vertically attached to horizontal walls of a cavity. The results indicated that the flow field and temperature distributions inside the cavity were strongly dependent on the Rayleigh numbers and the position of the heat sources. The results also indicated that the Nusselt number was an increasing function of the Rayleigh number, the distance between two heat sources, and distance from the wall and the average Nusselt number increased linearly with the increase in the solid volume fraction of nanoparticles

The LBM is an applicable method for simulating fluid flow and heat transfer [10–11]. This method was also applied to simulate the MHD [12] and, recently, nanofluid [13] successfully. The aim of the present study is to identify the ability of Lattice Boltzmann Method (LBM) for solving nanofluid, magnetic field simultaneously in the presence of a linear boundary condition. Moreover, the effect of magnetic field and its direction on the heat transfer in the cavity. In fact, it is endeavored to express the best situation for heat transfer and fluid flow with the considered parameters. Hence, the Al₂O₃-water nanofluid on laminar natural convection heat transfer at the presence of a magnetic field in linear temperature distribution on vertical side walls of the cavity by LBM was investigated.

The aim of the present study is to identify the ability of Lattice Boltzmann Method (LBM) for solving nanofluid,

magnetic field simultaneously in the presence of a linear boundary condition. Moreover, the effect of magnetic field and its direction on the heat transfer in the cavity.

2. Mathematical formulation

2.1 Problem statement

A two-dimensional square cavity is considered for the present study with the physical dimensions as shown in the **Fig. 1**. The bottom wall of the cavity is maintained at a uniform temperature and the top wall is insulated, the left and right vertical walls are heated linearly. The cavity is filled with water and Al_2O_3 nanoparticles. The nanofluid is Newtonian and incompressible. The flow is considered to be steady, two dimensional and laminar, and the radiation effects are negligible. The thermo-physical properties of the base fluid and the nanoparticles are given in **table 1**.

Table 1. Thermo-physical properties of water and nanoparticles

	ρ (kg/m ³)	C_p (J/kg K)	K (W/mK)	β (K ⁻¹)
Pure water	997.1	4179	0.613	21×10^{-5}
Al_2O_3	3970	765	40	0.85×10^{-5}

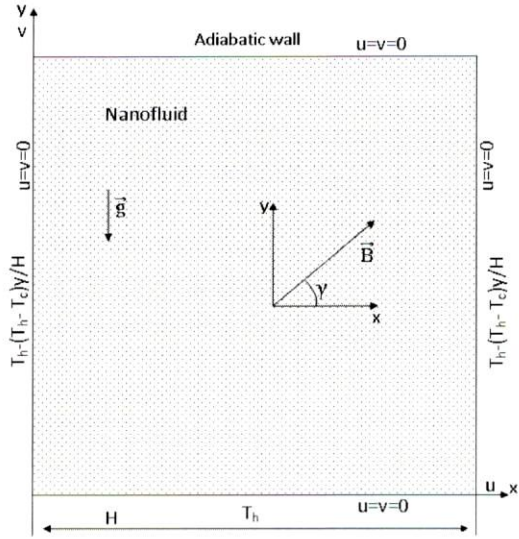


Fig.1 Geometry of the present study with boundary conditions

The density variation in the nanofluid is approximated by the standard Boussinesq model. The magnetic field strength B_0 is applied at an angle γ with respect to the coordinate system. It is assumed that the induced magnetic field produced by the motion of an electrically conducting fluid is negligible compared to the applied magnetic field. Furthermore, it is assumed that the viscous dissipation and Joule heating are neglected.

Therefore, governing equations can be written in dimensional form as follows:

$$\frac{\partial u}{\partial x} + \frac{\partial v}{\partial y} = 0 \quad (1)$$

$$\rho_{nf} \left(u \frac{\partial u}{\partial x} + v \frac{\partial u}{\partial y} \right) = -\frac{\partial p}{\partial x} + \mu_{nf} \left(\frac{\partial^2 u}{\partial x^2} + \frac{\partial^2 u}{\partial y^2} \right) + F_x \quad (2)$$

$$\rho_{nf} \left(u \frac{\partial v}{\partial x} + v \frac{\partial v}{\partial y} \right) = -\frac{\partial p}{\partial y} + \mu_{nf} \left(\frac{\partial^2 v}{\partial x^2} + \frac{\partial^2 v}{\partial y^2} \right) + F_y \quad (3)$$

$$u \frac{\partial T}{\partial x} + v \frac{\partial T}{\partial y} = \alpha_{nf} \left(\frac{\partial^2 T}{\partial x^2} + \frac{\partial^2 T}{\partial y^2} \right) \quad (4)$$

$$F_x = \frac{Ha^2 \mu_{nf}}{H^2} (v \sin \gamma \cos \gamma - u \sin^2 \gamma) \quad (5)$$

$$F_y = \frac{Ha^2 \mu_{nf}}{H^2} (u \sin \gamma \cos \gamma - v \cos^2 \gamma) + (\rho\beta)_{nf} g(T - T_m)$$

$$Ha = HB_0 \sqrt{\frac{\sigma_{nf}}{\mu_{nf}}} \quad (6)$$

The classical models reported in the literature are used to determine the properties of the nanofluid:

$$\rho_{nf} = (1 - \phi)\rho_f + \phi\rho_p \quad (7)$$

$$(\rho c_p)_{nf} = (1 - \phi)(\rho c_p)_f + \phi(\rho c_p)_p \quad (8)$$

$$(\rho\beta)_{nf} = (1 - \phi)(\rho\beta)_f + \phi(\rho\beta)_p \quad (9)$$

$$\alpha_{nf} = \frac{k_{nf}}{(\rho c_p)_{nf}} \quad (10)$$

In the above equations, ϕ is the solid volume fraction, ρ is the density, σ is the electrical conductivity, α is the thermal diffusivity, c_p is the specific heat at constant pressure and β is the thermal expansion coefficient of the nanofluid, γ is the direction of the magnetic field. The effective dynamic viscosity and thermal conductivity of the nanofluid can be modelled by:

$$\mu_{nf} = \frac{\mu_f}{(1 - \phi)^{2.5}} \quad (11)$$

$$k_{nf} = k_f \frac{k_p + 2k_f - 2\phi(k_f - k_p)}{k_p + 2k_f + \phi(k_f - k_p)} \quad (12)$$

The governing equations are subject to the following boundary conditions:

$$\begin{aligned} \text{Bottom wall} \quad & u = v = 0 \quad T(x, 0) = T_h \\ \text{Top wall} \quad & u = v = 0 \quad \left. \frac{\partial T}{\partial y} \right|_{y=H} = 0 \\ \text{Left wall} \quad & u = v = 0 \quad T(0, y) = T_h - (T_h - T_c) \frac{y}{H} \\ \text{Right wall} \quad & u = v = 0 \quad T(H, y) = T_h - (T_h - T_c) \frac{y}{H} \end{aligned} \quad (13)$$

2.2 Lattice Boltzmann Method

For the incompressible non isothermal problems, Lattice Boltzmann Method (LBM) utilizes two distribution functions, f and g , for the flow and temperature fields respectively.

For the flow field:

$$f_i(\mathbf{x} + \mathbf{c}_i \Delta t, t + \Delta t) = f_i(\mathbf{x}, t) - \frac{1}{\tau_v} (f_i(\mathbf{x}, t) - f_i^{\text{eq}}(\mathbf{x}, t)) + \Delta t F_i \quad (14)$$

For the temperature field:

$$g_i(\mathbf{x} + \mathbf{c}_i \Delta t, t + \Delta t) = g_i(\mathbf{x}, t) - \frac{1}{\tau_\alpha} (g_i(\mathbf{x}, t) - g_i^{\text{eq}}(\mathbf{x}, t)) \quad (15)$$

Where the discrete particle velocity vectors defined by \mathbf{c}_i , Δt denotes lattice time step which is set to unity. τ_v , τ_α are the relaxation time for the flow and temperature fields, respectively. f_i^{eq} , g_i^{eq} are the local equilibrium distribution functions that have an appropriately prescribed functional dependence on the local hydrodynamic properties which are calculated with Eqs.(16) and (17) for flow and temperature fields respectively.

$$f_i^{\text{eq}} = \omega_i \rho \left[1 + \frac{3(\mathbf{c}_i \cdot \mathbf{u})}{c^2} + \frac{9(\mathbf{c}_i \cdot \mathbf{u})^2}{2c^4} - \frac{3\mathbf{u}^2}{2c^2} \right] \quad (16)$$

$$g_i^{\text{eq}} = \omega_i' T \left[1 + 3 \frac{\mathbf{c}_i \cdot \mathbf{u}}{c^2} \right] \quad (17)$$

\mathbf{u} and ρ are the macroscopic velocity and density, respectively. c is the lattice speed which is equal to $\Delta x / \Delta t$ where Δx is the lattice space similar to the lattice time step Δt which is equal to unity, ω_i is the weighting factor for flow, ω_i' is the weighting factor for temperature. D2Q9 model for flow and D2Q4 model for temperature are used in this work so that the weighting factors and the discrete particle velocity vectors are different for these two models and they are calculated with Eqs (18-20) as follows:

For D2Q9

$$\omega_0 = \frac{4}{9}, \omega_i = \frac{1}{9} \text{ for } i = 1, 2, 3, 4 \text{ and } \omega_i = \frac{1}{36} \text{ for } i = 5, 6, 7, 8 \quad (18)$$

$$\mathbf{c}_i = \begin{cases} 0 & i = 0 \\ (\cos[(i-1)\pi/2], \sin[(i-1)\pi/2])c & i = 1, 2, 3, 4 \\ \sqrt{2}(\cos[(i-5)\pi/2 + \pi/4], \sin[(i-5)\pi/2 + \pi/4])c & i = 5, 6, 7, 8 \end{cases} \quad (19)$$

For D2Q4

The temperature weighting factor for each direction is equal to $\omega_i' = 1/4$.

$$\mathbf{c}_i = (\cos \cos[(i-1)\pi/2], \sin[(i-1)\pi/2])c \quad (20) \\ i = 1, 2, 3, 4$$

The kinematic viscosity ν and the thermal diffusivity α are then related to the relaxation time by Eq. (21):

$$\nu = \left[\tau_v - \frac{1}{2} \right] c_s^2 \Delta t \quad \alpha = \left[\tau_\alpha - \frac{1}{2} \right] c_s^2 \Delta t \quad (21)$$

Where c_s is the lattice speed of sound which is equals to $c_s = c / \sqrt{3}$. In the simulation of natural convection, the

external force term F appearing in Eq. (14) is given by Eq.(22)

$$F_i = \frac{\omega_i}{c_s^2} F \cdot \mathbf{c}_i \quad (22)$$

Where $F = F_x + F_y$

The macroscopic quantities, \mathbf{u} and T can be calculated by the mentioned variables, with Eq.(23-25).

$$\rho = \sum_i f_i \quad (23)$$

$$\rho \mathbf{u} = \sum_i f_i \mathbf{c}_i \quad (24)$$

$$T = \sum_i g_i \quad (25)$$

2.2 Non-dimensional parameters

By fixing Rayleigh number, Prandtl number and Mach number, the viscosity and thermal diffusivity are calculated from the definition of these non dimensional parameters. $\nu_f = N.Ma.c_s \sqrt{\text{Pr}/\text{Ra}}$ Where N is number of lattices in y -direction. Rayleigh and Prandtl numbers are defined as $\text{Ra} = g\beta_f H^3 (T_h - T_c) / \nu_f \alpha_f$ and $\text{Pr} = \nu_f / \alpha_f$, respectively.

Mach number should be less than $Ma = 0.3$ to insure an incompressible flow. Therefore, in the present study, Mach number was fixed at $Ma = 0.1$. Nusselt number is one of the most important dimensionless parameters in the description of the convective heat transport. Nusselt number is one of the most important dimensionless parameters in the description of the convective heat transport. The local Nusselt number and the average value at the bottom and the right walls are calculated as:

$$\text{Nub}_{\text{loc}} = - \frac{k_{nf}}{k_f} \frac{H}{T_h - T_c} \frac{\partial T}{\partial y} \Big|_{y=0} \quad (26)$$

$$\text{Nur}_{\text{loc}} = - \frac{k_{nf}}{k_f} \frac{H}{T_h - T_c} \frac{\partial T}{\partial x} \Big|_{x=H}$$

$$\text{Nub} = \frac{1}{H} \int_0^H \text{Nub}_{\text{loc}} dx \quad (27)$$

$$\text{Nur} = \frac{1}{H} \int_0^H \text{Nur}_{\text{loc}} dy$$

3. Results and discussion

3.1 Validation of the numerical code

Lattice Boltzmann Method scheme was utilized to obtain the numerical simulations in a cavity with a linear boundary condition that is filled with nanofluid of water/ Al_2O_3 . **Fig. 2** demonstrates the effect of grid resolution and the lattice sizes (20x20), (40x40), (60x60), (80x80) and (100x100) for $\text{Ra} = 10^5$, $\text{Ha} = 0$ and $\phi = 0$ by calculating the average Nusselt number on the bottom and right walls, it was found that a grid size of (100x100) ensures a grid independent solution. In order to check on the accuracy of the numerical technique

employed for the solution of the considered problem, the present numerical code was validated with the published study of Ghasemi et al [14] (Fig.3). it shows the dimensionless temperature along the horizontal axial midline of the enclosure for three values of the Hartmann number, for $Ra=10^5$ and for a solid volume fraction $\phi = 0.03$, excellent agreement is also found.

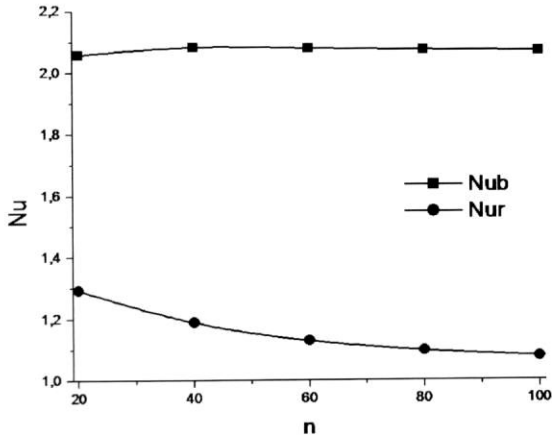


Fig. 2. Average Nusselt number on bottom and right walls for different uniform grids ($\phi = 0$, $Ra=10^5$ and $Ha=0$)

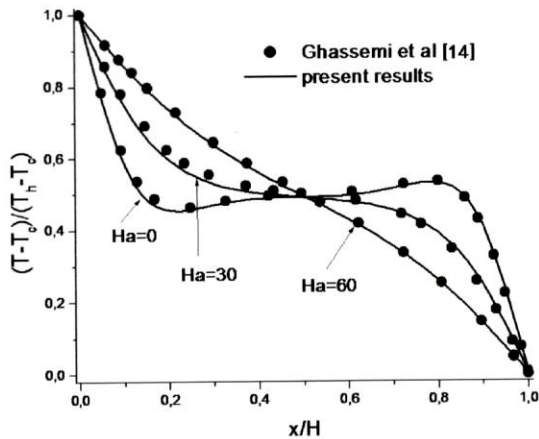


Fig. 3 Comparison of the temperature on axial midline between the present results and numerical results by Ghassemi et al. [14] ($\phi = 0.03$, $Ra=10^5$)

3.2 Results and discussion

Fig.4 presents the variation of the maximum value of the stream function as a function of Hartman number for several values of Rayleigh number for $\phi = 0$ and $\gamma = 0^\circ$. It is observed that the effect of Hartmann number is opposite to the effect of Rayleigh number. For $Ra = 10^3$ and 10^4 , $|\psi|_{max}$ is constant and small for all values of Hartmann number. The conduction is dominant. For $Ra = 5 \times 10^4$ and 10^5 , the convection is dominant for low values of Hartmann number, more than the

Hartmann number increases convection is more disadvantaged, until reaching the conductive regime.

Fig.5 show the average Nusselt number on the bottom wall, the increase of Rayleigh number increases the heat transfer rate, on the contrary, the increase of the Hartmann decreases the heat transfer rate.

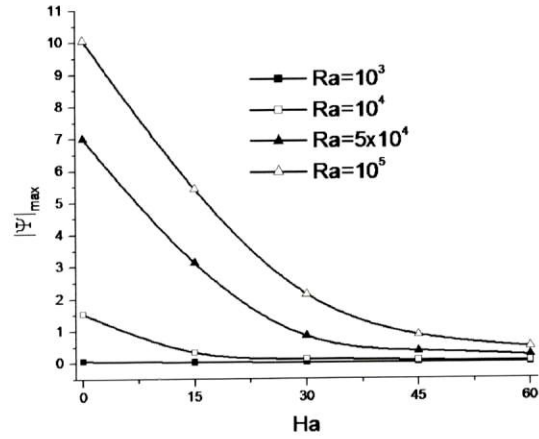


Fig.4 Variation of the maximum of stream function with Hartmann number for different Rayleigh number for $\gamma = 0^\circ$ and $\phi = 0$

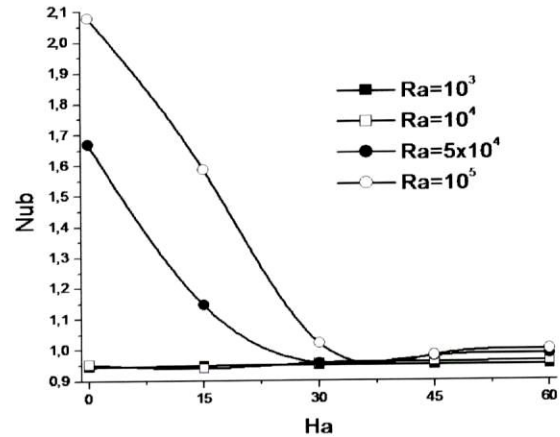


Fig.5 Variation of the average Nusselt number on the bottom wall with Hartmann number for different Rayleigh number for $\gamma = 0^\circ$ and $\phi = 0$

Fig. 6 presents the effect of Hartmann number and solid volume fraction on the Nusselt number at $Ra = 5 \times 10^4$ and $\gamma = 0^\circ$. At small values of Hartmann number ($Ha < 5$), the addition of nanoparticles augments the heat transfer, but if Hartmann number increases ($5 < Ha < 15$) the addition of nanoparticles does not have a significant effect. For $Ha > 15$ the heat transfer is obviously increase as the solid volume fraction increases.

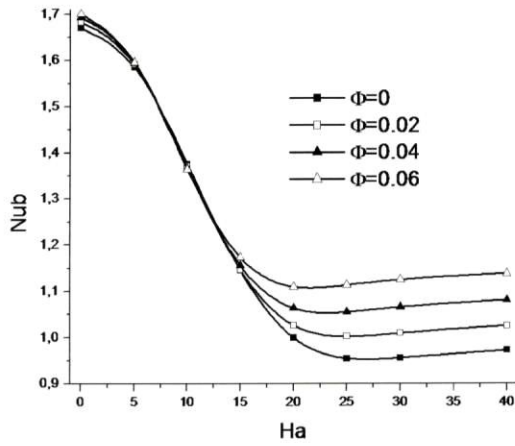


Fig.6 Variation of the average Nusselt number on the bottom wall with Hartmann number for different volume fraction for $\gamma = 0^\circ$ and $Ra=5 \times 10^4$

Figs .7 present the effect of the direction of the magnetic field and solid volume fraction on the Nusselt number at $Ra=5 \times 10^4$ and for several Hartmann number. At low Hartmann number ($Ha=5$), for all γ , the addition of nanoparticles augments the heat transfer at the bottom of the cavity. For $Ha \geq 15$, it is observed that the magnetic field direction controlled the effect of nanoparticles in the fluid. For the bottom wall, the heat transfer decreases by the addition of nanoparticles ($60 < \gamma < 120$) and increases by the addition of nanoparticles for the rest of the range of γ . This behavior becomes more significant for $Ha = 30$.

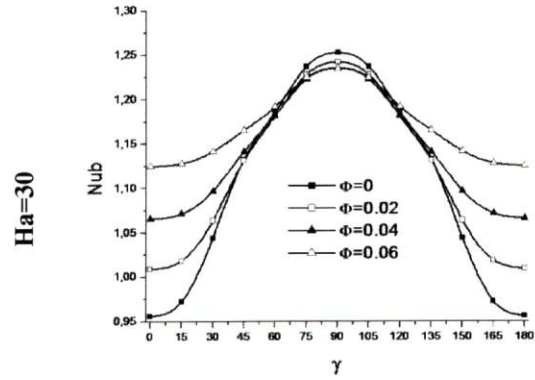
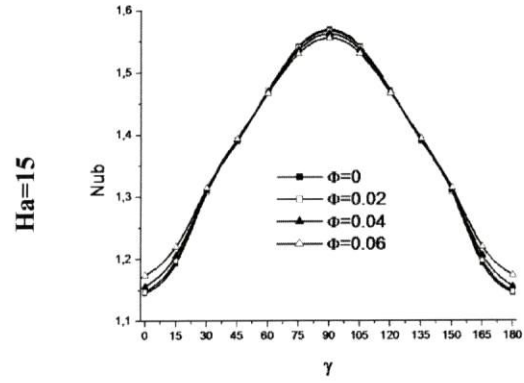
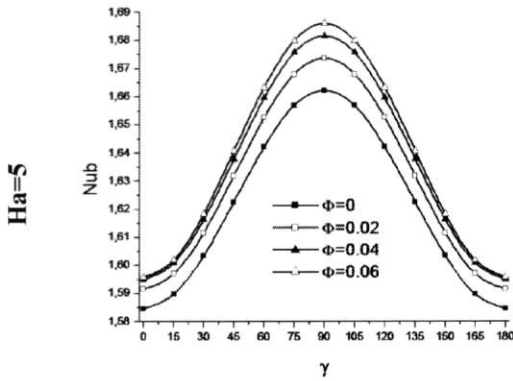


Fig.7 Variation the average Nusselt number on the bottom wall with γ for different Hartmann number and volume fraction for $Ra=5 \times 10^4$



4. Conclusions

In this paper the effects of a magnetic field on nanofluid flow in a cavity with a linear boundary condition has been analyzed with Lattice Boltzmann Method. This study has been carried out for the pertinent parameters in the following ranges: the Rayleigh number of base fluid, $Ra=10^3-10^5$, Hartmann number of the magnetic field between 0 and 60, the volume fraction is from $\phi = 0$ to 0.06 and the direction of the magnetic field in the range $0^\circ < \gamma < 180^\circ$

Nomenclature

B	Magnetic field (Tesla)
c	Lattice speed (ms^{-1})
c_s	Speed of sound (ms^{-1})
c_i	Discrete particle speeds (ms^{-1})
c_p	Specific heat at constant pressure (JK^{-1})
F	External forces ($kg\ m\ s^{-2}$)
f	Density distribution functions (kgm^{-3})
f^{eq}	Equilibrium density distribution functions (kgm^{-3})
g	Internal energy distribution functions (K)
g^{eq}	Equilibrium internal energy distribution (K)
g_i	Gravity vector ($m\ s^{-2}$)
Ha	Hartmann number
k	thermal conductivity ($Wm^{-1}K^{-1}$)

Ma	Mach number
Nu	Local Nusselt number
Pr	Prandtl number
Ra	Rayleigh number
T	Temperature (K)

Greek symbols

Δx	Lattice spacing (m)
Δt	Time increment (s)
τ_a	Relaxation time for temperature (s)
τ_v	Relaxation time for flow (s)
ν	Kinematic viscosity ($\text{m}^2 \text{s}^{-1}$)
α	Thermal diffusivity ($\text{m}^2 \text{s}^{-1}$)
ρ	Fluid density (kgm^{-3})
σ	electrical conductivity ($\Omega^{-1} \text{m}^{-1}$)
ψ	Non-dimensional stream function
Φ	Solid volume fraction

References

1. S. Ostrach, Natural convection in enclosures, *Journal of Heat Transfer*, vol 110, pp. 1175-1190, 1988.
2. M. Moreau, *Magnetohydrodynamics*, Kluwer Academic Publishers, The Netherlands, 1990.
3. H. Ozoe, K. Okada, The effect of the direction of the external magnetic field on the three dimensional natural convection in a cubical enclosure, *International Journal of Heat and Mass Transfer*, vol. 32, pp. 1939-1954, 1989
4. Y. Al-Badawi and H. M. Duwairi . MHD Natural Convection in Iso-Flux Enclosures Filled With Porous Medium. *Int. J. Heat Technol.* Vol. 28 (2), pp. 87-91, 2010.
5. S. Abishek and S. S. Katte. Magnetohydrodynamic thermo-solutal buoyant darcy convection in a square enclosure. *Int. J. Heat Technol.*, vol. 28(2), pp. 105-116, 2010.
6. E. Fattahi, M. Farhadi, K. Sedighi, H. Nemati, Lattice Boltzmann simulation of natural convection heat transfer in nanofluids, *International Journal of Thermal Sciences*, vol. 52, pp. 91-101, 2012
7. G.H.R. Kefayati, S.F. Hosseinizach, M. Gorji, H. Sajjadi, Lattice Boltzmann simulation of natural convection in tall enclosures using water/SiO₂ nanofluid, *International Communications in Heat and Mass Transfer*, vol. 38, pp. 798-805, 2011
8. F. Lai, Y. Yang, Lattice Boltzmann simulation of natural convection heat transfer of Al₂O₃/water nanofluids in a square enclosure, *International Journal of Thermal Sciences*, vol. 50, pp. 1930-1941, 2011.
9. A.H. Mahmoudi, M. Shahi, A.M. Shahedin, N. Hemati, Numerical modeling of natural convection in an open cavity with two vertical thin heat sources subjected to a nanofluid, *International Communications in Heat and Mass Transfer*, vol.38, pp.110-118,2011.
10. H. Nemati, M. Farhadi, K. Sedighi, M.M. Pirouz, E. Fattahi, Numerical simulation of fluid flow around two rotating side by side circular cylinders by Lattice Boltzmann method, *International Journal of Computational Fluid Dynamics* vol. 24, pp. 83-94, 2010.
11. M. Mehravaran, S.K. Hannani, Simulation of buoyant bubble motion in viscous flows employing lattice Boltzmann and level set methods, *Scientia Iranica*, vol. 18, pp. 231-240, 2011
12. D. Martinez, S. Chen, W.H. Matthaeus, Lattice Boltzmann magneto hydrodynamics, *Physics of Plasmas*, vol. 1, pp. 1850-1867, 1994
13. H. Nemati, M. Farhadi, K. Sedighi, E. Fattahi, A.A.R. Darzi, Lattice Boltzmann simulation of nanofluid in lid-driven cavity, *International Communications in Heat and Mass Transfer*, vol. 37, pp.1528-1534, 2010.
14. B. Ghasemi, S.M. Aminossadati, A. Raisi, Magnetic field effect on natural convection in a nanofluid-filled square enclosure, *International Journal of Thermal Sciences* vol.50, pp. 1748-1756, 2011.